PCCP

Accepted Manuscript




ROYAL SOCIETY OF CHEMISTRY

www.rsc.org/pccp

PCCP

Dynamic Article Links ►

Cite this: DOI: 10.1039/c0xx00000x

www.rsc.org/

PAPER

# Cu (II)-alkyl amines complex mediated hydrothermal synthesis of Cu nanowires: Exploring the dual role of alkyl amines

D.V. Ravi Kumar, Inhyuk Kim, Zhaoyang Zhong, Kyujin Kim, Daehee Lee, and Jooho Moon*

***Received (in XXX, XXX) Xth XXXXXXXXX 20XX, Accepted Xth XXXXXXXXX 20XX***

**DOI: 10.1039/b000000x**

Ligands/surfactants play an important role in the synthesis of anisotropic nanomaterials. Other than site specific binding to the crystal plane, they can also undergo complexation with metal ions, altering the nature of the metal complex. The ligand-metal complex formation could be sufficient to modify the reaction kinetics and could affect the size and morphology of the nanostructures. In this article, we investigated such a change of the metal precursor caused by ligands (i.e., alkyl amines) in the hydrothermal synthesis of Cu nanowires in the presence of glucose as a reducing agent. Comparative studies were carried with other nitrogen-based surfactants such as cetyl trimethyl ammonium bromide and polyvinyl pyrrolodine. Our experimental results confirmed the complex formation of $Cu^{2+}$ ions with alkyl amines and its application for nanowire synthesis. Slow reduction of this complex allows for the generation of twinned seeds which are later grown to nanowires by consuming newly generated seeds in the presence of excess alkyl amine.

PCCP

Dynamic Article Links ►

Cite this: DOI: 10.1039/c0xx00000x

www.rsc.org/

PAPER

## Introduction

One-dimensional noble metal nanostructures such as wires are interesting candidates not only because of their topology but also due to their properties such as surface plasmon resonance (SPR), enhanced catalytic activity, and their thermal and electrical properties at the nanoscale.[1-4] Metal nanowires have been proved as efficient materials for the fabrication of transparent, flexible electrodes with a low sheet resistance and high transparency, which are comparable to indium tin oxide (ITO).[5] Henceforth, they can replace the high cost and brittle ITO used in the fabrication of transparent electrodes (TEs). In addition to this, metal nanowires have also been explored as potential candidates for applications such as catalysts, enzyme-free sensors, and surface enhanced Raman scattering (SERS).[3,6-7] As compared to other noble metals, Cu is much cheaper, a highly abundant element in the earth's crust, and the conductivity of Cu is is acceptably close to that of Ag. Hence, Cu nanowires offer a low cost alternative to other noble metal nanowires and have become attractive materials in recent years for several applications.

However, Cu nanowires have been scarcely reported in literature compared to other metal nanowires such as Ag and Au.[8-10] The parameters of high quality nanowires such as the aspect ratio and amount of particles associated with the wires depends on several reaction conditions such as the nature of metal salts,[8] concentration and nature of seeds,[9] reaction temperature, and stirring speed.[10] Existing reports on the synthesis of Cu nanowires are limited to the synthesis of Cu nanowires followed by the fabrication of TEs while very few studies address the above mentioned issues. The important synthetic methods used to produce Cu nanowires can be summarized as the hydrothermal reduction of Cu salts in the presence of alkyl amines,[11] reduction of copper salts using a mild

reducing agent such as glucose in the addition of alkyl amines,[12-13] reduction of copper salts using toxic hydrazine with ethylene diamine (EDA),[14-15] and catalytic reduction of Cu salts in the presence of other metals such as Ni and Pt.[16-18] Among these methods, the synthesis of Cu nanowires using glucose as a reducing agent with alkyl amines is known to yield very thin (~25 nm diameter) and ultra-long wires (hundreds of microns long). This aspect ratio is very high compared to nanowires produced by other methods such as the hydrazine reduction method (80–90 nm diameter and ~60 microns long) and catalytic reduction methods (~80 nm diameter and ~40 microns long). Very recently, the large scale synthesis of Cu nanowires was reported using a pressure cooker,[19] which is similar to the concept of the hydrothermal method. This clearly implies that hydrothermal methods are capable of yielding ultra-long copper nanowires with a scalable quantity.

Ligands are known to play an important role in the size selective/shape selective synthesis of nanomaterials.[20] They stabilize nanoparticles in various environments by effectively capping the nanoparticle core.[21] In anisotropic nanoparticle synthesis, it is believed that the ligands induce anisotropy by site specific binding to some of the crystal facets of the nanoparticles.[22-24] Other than common approaches such as site specific binding, ligands also play a critical role in the nanoparticle formation, which is often overlooked. The ligands may undergo complexation with metal ions or change the nature of the precursor metal complex, which subsequently affects the pH of the reaction medium and the reduction potential of the metal. These changes can influence the reaction kinetics and may show a dramatic effect on the final size/morphology of the resulting nanocrystals.[25] Similar to other noble metals, the roles of ligands or capping agents are not clearly understood in the synthesis of Cu nanowires. For example, Zeng *et al.*[14] reported the synthesis of Cu nanowires using hydrazine and EDA, which was modified by Wiley and co-workers.[15] It is believed that EDA acts as a capping agent in this process. Jin *et al*. also studied the synthesis of Cu nanowires by the same method and explained the growth of nanowires by screw dislocations in which the role of EDA was assigned as a complex agent rather than a capping agent.[26]

Mohl *et al*. demonstrated the single crystalline nature of the Cu nanowires synthesized by a hydrothermal method in the presence of hexadecylamine (HDA) as a capping agent and glucose as a reducing agent.[12] Xia and co-workers obtained a pentagonal twinned nature of the Cu nanowires when synthesized under the same capping and reducing agents.[13] This clearly shows that the role of HDA is also unclear in the synthesis of Cu nanowires.

In the typical hydrothermal process, when alkyl amine is added to the $CuCl_2$ solution, it turns blue upon stirring, which could be due to the formation of a Cu(II)-alkyl amine complex. As mentioned earlier, the formation of anisotropic structures depends on the initial nature of the complex and alkyl amine may play a role additional to site specific binding. This requires the need to understand the role of alkyl amines and their complex formation with copper ions. Although few reports have discussed the hydrothermal synthesis of Cu nanowires, understanding of the formation mechanism of nanowires, the role of alkyl amines, and their complex formation with $Cu^{2+}$ ions is lacking in the literature. In the study, we investigated the role of Cu(II)-alkyl amine complex formation in the hydrothermal synthesis of Cu nanowires. The alkyl amines studied include HDA, octadecyl amine (ODA), and oleyl amine (OLA). We also performed a comparative study with the nitrogen-containing ligands of polyvinyl pyrrolidine (PVP) and cetyl trimethyl ammonium bromide (CTAB).

## Experimental

### *Synthesis*

Anhydrous $CuCl_2$ (97%), dextrose, HDA (98%), ODA (97%), and OLA (98%) were obtained from Sigma-Aldrich Chemicals. Hexane and isopropanol were obtained from Duksan Pure Chemicals. All of the chemicals were used as received without further purification. We utilized a hydrothermal method for the synthesis of the Cu nanowires.[12] Initially, 50 mL of an aqueous solution containing anhydrous $CuCl_2$ (0.013 M), glucose (0.011 M), and HDA (0.056 M) was stirred vigorously at room temperature overnight to obtain a blue emulsion. Then, the

emulsion was transferred to a 120 mL capacity Teflon-lined autoclave (acid digestion vessel, Model-4748, Parr Instruments). The precursor solution was heated at 120°C for 24 h. After completion of the reaction, the autoclave was cooled to room temperature and the reddish brown product was collected in a separate vial. The products were washed successively with water, isopropanol, and hexane 2 or 3 times to remove unreacted impurities and excess alkyl amine. Finally, the precipitate was re-dispersed in isopropanol. The same procedure was repeated for the synthesis of Cu nanowires using either ODA or OLA instead of HDA. All other experiment conditions such as the reaction temperature, reaction time, alkyl amine to Cu (II) molar ratio, and glucose concentration were unaltered.

***Characterizations***

The purified Cu nanowires dispersed in isopropanol, Cu(II)-alkyl amine complexes, and $CuCl_2$ solution with other surfactants such as CTAB and PVP were characterized using a UV-vis spectrophotometer (V-530, Jasco). The Cu(II) complexes with different alkyl amines were also characterized by a FT-IR spectrophotometer (Vertex 50, Bruker). For the X-ray diffraction (XRD) measurements, Cu nanowires were coated on a glass slide and vacuum dried to form Cu nanowire films. The obtained films were characterized using an X-ray diffractometer (ME 200 DX, Rigaku). A Cu nanowire dispersion in isopropanol was drop-cast on either a clean Si wafer or Cu grid for electron microscope characterization. A field emission scanning electron microscope (FESEM, JEOL-6701, JEOL) operated at 20 kV was utilized to monitor the morphologies of the Cu nanowires synthesized with different ligands. A high resolution transmission electron microscope (HRTEM, JEM-ARM 200F, JEOL) operated at 200 kV was used to characterize the Cu nanowires.

## Results and discussion

Cu nanowires were synthesized using three different alkyl amines and glucose as a reducing agent under hydrothermal conditions. Glucose was used as an external reducing agent to assist the rapid synthesis of Cu nanowires at a temperature lower than that in earlier reported methods using ODA[11,27] and OLA.[28] Fig. 1 shows SEM images of the Cu nanowires synthesized using the different alkyl amines of HDA, ODA, and OLA. In all of these cases, the obtained nanowires are ultra-long (hundreds of microns long) (Fig. 1a-b, 1d-e, and 1g-h, respectively) and the diameter of the wires varied from 20 to 40 nm (Fig. 1c, 1f, and 1i, respectively). Side views of the nanowires are shown in the insets of Fig. 1b and 1h, showing the pentagonal ends of the nanowires. Similar to the nanowires synthesized using HDA, the nanowires obtained using ODA and OLA also had a tendency to form bundles, aggregates, and kinks. In all three cases, although the major product is identified as nanowires, a few particles are associated with the nanowires (Fig. 1b, 1e, and 1h). These particles can be easily separated by the cross-flow filtration method suggested in previous reports.[29] For suitable comparison of the nanowires obtained using the different alkyl amines, the alkyl amine to $Cu^{2+}$ molar ratio was held constant. As the carbon chain length increased from HDA (contains 16 carbons in the alkyl chain) to ODA (contains 18 carbons in the alkyl chain) and OLA (contains 18 carbons in the alkyl chain and a double bond), the solubility of alkyl amine in water decreases. The relative decrease of the solubility of alkyl amine may diminish the local concentration of the capping agent. This situation would be unfavorable for the stabilization of initial seeds against phenomenon such as oxidative etching[30] and the seeds likely grow to nanoparticles and nanocubes. Hence, a relatively large number of nanoparticles and nanocubes coexist with nanowires synthesized using ODA and OLA (Fig. 1e and 1h). Moreover, nanocubes associated with Cu nanowires are high in number in the case of the nanowires synthesized using OLA (Fig. **1h**). This observation is also supported by XRD results for the nanowires synthesized using OLA. The XRD patterns of Cu nanowires synthesized using the different alkylamines are shown in Fig. 2a. Unlike the

patterns obtained for the cases of HDA and ODA, the diffraction patterns of the Cu nanowires synthesized with OLA demonstrate (111) and (200) peaks with similar intensities. Cu nanocubes are known to have preferred orientation with {100} planes, exhibiting a (200) peak with a higher intensity than (111).[13,31] As observed in the SEM images, relatively large numbers of Cu nanocubes contained in the nanowires under OLA would increase the intensity of the (200) peak. Three different Cu nanowire dispersion inks are shown in the inset and their UV-vis spectra are presented in Fig. **2b**. UV-vis spectra of Cu nanowire inks from three different alkyl amines of HDA, ODA, and OLA have different maximum absorption peaks at 568, 580, and 572 nm, respectively, even though they are consisted of the same copper element. The SPR effect of the copper nanowire can be changed by their diameter and the average diameter of copper nanowires using HDA, ODA and OLA are 24, 33,AD and 30 nm, respectively. Therefore the absorption maximum peak for each alkyl amine shows the different value.

HRTEM images of the nanowires synthesized using HDA are shown in Fig. 3a. The side-view of the penta-twinned end portion of the wire can be seen in Fig. 3b and the stem of a single wire is observed in Fig. 3c. The interplanar spacing of 0.21 nm corresponds to the (111) plane of FCC copper (Fig. 3d), suggesting the [110] growth direction of the wire.[28] A kink of the wire can be also seen in Fig. 3e and 3f, revealing the presence of (111) planes and a twin boundary. This kind of twin is not observed in the single crystalline nanowire, which also indicates that the pentagonal nanowires could be generated from the twinned seeds. HRTEM images of the nanowires synthesized using ODA also show similar features, confirming the same capping action of different alkyl amines (Fig. 4).

To understand the nature of the seeds generated from alkyl amines, we collected aliquots of the different samples synthesized using HDA and ODA after reaction for 3 h. Fig. 5a and b show the HRTEM images of the seed particles generated from the different alkyl amines where the particle sizes are in the

range of 3−8 nm. The majority of these particles produced in the presence of HDA are multi-twinned (Fig. 5c) and the corresponding fast Fourier transform (FFT) of a single particle is shown in Fig. 5d. To obtain the crystal structure with minimal distortion, the reciprocal lattice points of the FFT of the twinned particle were masked (Fig. 5e) and inverted (Fig. 5f). The (111) and (200) patterns are indexed according to FCC of Cu (Fig. 5g and 5h). The FFT image of the single particle is magnified and indexed in Fig. 5g and 5h, respectively. This image analysis reveals the (111) and (200) planes of the copper seed particles. Our HRTEM analysis results are in good agreement with the simulated Cu decahedron structures reported by Pileni and coworkers,[32] which is clearly indicative of the penta-twinned nature of the seed particles.[33-34] It is known that the observed multi-twinned particles at the initial stages of reaction can grow larger in size with penta-twinned top and bottom facets containing (111) planes and (100) planes at the sides.[28,35] Instead of forming fully grown decahedron beyond the critical size in the latter stages of the growth process, the penta-twinned seeds prefer to grow along the parallel axis to avoid stain.[33] Capping agents (in the present case, alkyl amines) serve as external confinement, stabilizing the {100} side facets and inhibiting lateral growth.[36] This hypothesis can be supported by experimental and theoretical investigations in which well-known capping agents such as CTAB and PVP are involved in the synthesis.[37-41] However, in the case of an alkyl amine such as HDA, no such evidences are available in the literature. Pencil-like pentagonal rods with micron-sized widths are observed when the HDA concentration was decreased to half of its original concentration (Fig. 6). Due to the poor passivation of side {100} facets at a low surfactant concentration, newly formed seeds can grow on the side facets, resulting in Cu rods with micron-sized widths instead of nanowires. This observation confirms the selective adsorption of alkyl amines on {100} facets, inhibiting the growth in the lateral direction and suggesting that alkyl amines serve as external confinements for one-dimensional growth of the nanowires.

Well-known capping agents such as CTAB and PVP are known to control the growth habits of crystal

facets by selective adsorption and to successfully generate the anisotropic structures of Au and Ag. Hence, we carried out experiments by replacing HDA with either CTAB (the surfactant to copper ion concentration ratio was kept the same in the cases of HDA and CTAB) or PVP (since PVP is a polymer, instead of the concentration ratio, we maintained the same weight %) for the synthesis of Cu nanowires in which glucose is used as a reducing agent. It is worthwhile to mention that both CTAB and HDA have the same carbon chain length. The difference arises from the nitrogen in CTAB, which is a quaternary ammonium salt, whereas HDA is a primary amine. We did not observe the formation of nanowires when the alkyl amines were replaced with CTAB and PVP under similar reaction conditions. This finding clearly implies that the capping action of surfactant is not sufficient for successful generation of nanowires, but rather the formation of multi-twinned seeds, which provide internal confinement for the growth of nanowires, is most important. The seeds can be either added externally, as in the case of gold nanorod synthesis,[42] or *in situ* generated by employing suitable reaction conditions, as in the case of the polyol synthesis of Ag nanowires in which alkyl amines play an important role in the self-seed generation, leading to directional growth.[43] In the typical synthesis of Cu nanowires using HDA, a blue colored emulsion was evolved after vigorous stirring of the HDA-added aqueous solution of Cu salt, as shown in the inset in Fig. 7a. The evolution of the blue color suggests a considerable change in the initial nature of the metal precursor after the addition of HDA. To understand this change in detail, we tested other alkyl amines including ODA and OLA, both of which also resulted in a blue-colored emulsion when added to the $Cu^{2+}$ solution (inset of Fig. 7b), which eventually led to the synthesis of Cu nanowires after hydrothermal treatment of the blue emulsions. The formation of the blue-colored emulsion of alkyl amines with $Cu^{2+}$ ions was further investigated by evaluating the visible spectra of the aqueous Cu salt solutions with and without HDA. The $Cu^{2+}$ aqueous solution shows a peak at 811 nm and the peak position was not altered by the presence of glucose (Fig. 7a). After the addition of HDA to the $Cu^{2+}$

aqueous solution, the peak position shifted from 811 nm to 595 nm. Similarly, broad peaks at 633 nm and 617 nm were observed with ODA and OLA, respectively (Fig. 7b). These spectral results agree well with previous studies of aqua and amine complexes of Cu(II),[44-45] suggesting aqua and amine complex natures of the $Cu^{2+}$ ions before and after the addition of alkyl amines (Fig. 7c). However, such drastic color changes and corresponding spectral changes were not detected in the cases of CTAB and PVP.

When there are no ligands present in the aqueous Cu ion solution, $Cu^{2+}$ ions may be coordinated with either $H_2O$ or $Cl^-$ ligands and the solution is cyan-colored. The origin of this color can be attributed to *d-d* transitions which generally occur in transition metal complexes. Changes of the ligand environment, geometry of the complex, and position of the ligand can considerably affect the splitting of *d* orbitals, which is responsible for the *d-d* transitions.[46] When alkyl amine is added to a Cu aqueous solution, a lone pair on nitrogen can effectively coordinate with Cu ions. This successfully replaces weak $H_2O$ or $Cl^-$ ligands, forming a blue-colored $Cu^{2+}$-amine complex. The change in the ligand environment would be sufficient to induce the splitting of the *d* orbital and hence, the corresponding spectral changes. However, a lone pair is not available on nitrogen in the case of CTAB. Nitrogen in the monomer of PVP is 3° amine and the lone pair on nitrogen may be delocalized due to the presence of the adjacent –C=O group. In addition to this, unlike alkyl amines, PVP is completely soluble in water and the lone pair on nitrogen would be involved in hydrogen bonding with water molecules. Therefore, the lone pair on nitrogen in PVP is not readily available to coordinate with $Cu^{2+}$ ions and in turn, CTAB and PVP could not form a suitable precursor complex from which penta-twinned seeds are generated by the slow reduction of the metal complex.

Cu(II)-alkyl amine complex formation was further investigated by evaluating the FT-IR spectra. Fig. 8 shows the FT-IR spectra of free alkyl amines and Cu(II)-alkyl amine complexes. The FT-IR spectrum of HDA reveals a peak at 3,334 $cm^{-1}$, confirming the typical nature of HDA.[47] This peak intensity was

considerably decreased after forming the complex with $Cu^{2+}$ ions. Instead of the two peaks observed at 1,573 and 1,645 $cm^{-1}$ in free HDA (attributed to the deformations of the amine group),[47-48] a relatively broad peak was detected at 1,639 $cm^{-1}$ after the complex formation with $Cu^{2+}$ ions (Fig. 8a). Similarly, in the case of ODA and OLA, the intensity of the N-H stretching mode[48] observed in the region of 3,300−3,100 $cm^{-1}$ in the free alkyl amines was considerably diminished in the Cu(II)-alkyl amine complex. The peak at 1,605 $cm^{-1}$ attributed to N-H bending vibrations[48] in free ODA was also shifted to 1,635 $cm^{-1}$ after the complex formation with $Cu^{2+}$ ions. In the case of free OLA, the two peaks present at 1,575 $cm^{-1}$ and 1,620 $cm^{-1}$ can be assigned to C=C and N-H bending vibrations, respectively.[47-48] In the $Cu^{2+}$-OLA complex, we observed one broad peak at 1,638 $cm^{-1}$ instead of two peaks. In addition, the intensities of the C-H stretching peaks observed in the region of 2,900−2,800 $cm^{-1}$ were considerably decreased after complex formation of alkyl amines with $Cu^{2+}$ ions in all three cases (Fig. 8b and 8c). From these spectroscopic investigations, it can be concluded that alkyl amines are capable of forming a complex with copper ions and this complex could be a suitable metal precursor for the self-seed generation required for nanowire growth. The dual role of alkyl amines in the hydrothermal synthesis of Cu nanowires is visualized in Fig. 9. In the initial stages of the reaction, alkyl amines act as a complexing agent by forming a suitable metal complex for self-seed generation. Slow reduction of this complex allows for the generation of twinned seeds which are later grown to nanowires by consuming newly generated seeds. In the latter stages of the reaction, the alkyl amines play an additional role as a capping agent by selective adsorption on newly generated seeds, allowing them to grow into nanowires. In the absence of sufficient alkyl amine, however, pencil-like pentagonal rods with micron-sized widths are observed due to the lack of external confinement for one-dimensional growth.

## Conclusions

We investigated the role of ligands/capping agents in the hydrothermal synthesis of Cu nanowires by utilizing alkyl amines (HDA, ODA, and OLA) as capping agents and glucose as a reducing agent. The alkyl amines stabilize the {100} facets of the twinned seeds and restrict their lateral growth, serving as external confinements for one-dimensional growth. Hence, ultra-long nanowires were synthesized in all of the cases involving excess alkyl amines. If the amount of alkyl amines was insufficient, we obtained pencil-like pentagonal rods with micron-sized widths. Due to the poor passivation of side {100} facets, newly formed seeds can grow on the side facets, resulting in thick Cu rods instead of nanowires. On the other hand, nanowire formation was not observed when the synthesis was conducted in the presence of CTAB and PVP, although they are also known to stabilize penta-twinned seeds. This clearly indicates that, in addition to their capping action, alkyl amines play an additional role by forming a blue-colored Cu(II)-alkyl amine complex. This complex formation is mandatory for the generation of penta-twinned seeds from which the nanowires are allowed to grow.

## Acknowledgements

We received financial support from a National Research Foundation of Korea (NRF) grant funded by the Korea government (MSIP) (No. 2012R1A3A2026417). This research was also partially supported by the third Stage of Brain Korea 21 Plus Project.

## Notes and references

*Department of Materials Science and Engineering, Yonsei University, 50 Yonsei-ro Seodaemun-gu, Seoul 120-749, Republic of Korea. Fax: +82-2-312-5375; Tel.: +82-2-2123-2855; E-mail: jmoon@yonsei.ac.kr*

1. J. Chen, B. J. Wiley and Y. Xia, *Langmuir*, 2007, **23**, 4120-4129.
2. X. Hou, X. Zhang, S. Chen, Y. Fang, N. Li, X. Zhai and Y. Liu, *Colloids Surf. A,* 2011, **384**, 345-351.
3. Z. Chen, A. R. Rathmell, S. Ye, A. R. Wilson and B. J. Wiley, *Angew. Chem.,* 2013, **125**, 13953-13956.

4. S. Wang, Y. Cheng, R. Wang, J. Sun and L. Gao, *ACS Appl. Mater. Interfaces* 2014, **6**, 6481-6486.

5. J.-Y. Lee, S. T. Connor, Y. Cui, and P. Peumans, *Nano Lett.* 2008, **8**, 689-692.

6. S. J. Lee, A. R. Morrill and M. Moskovits, *J. Am. Chem. Soc.* 2006, **128**, 2200-2201.

7. U. Yogeswaran and S.-M. Chen, *Sensors* 2008, **8**, 290-313.

8. B. Jia, M. Qin, Z. Zhang, A. Chu, L. Zhang, Y. Liu and X. Qu, *J. Mater. Sci* 2013, **48**, 4073-4080.

9. Y. Sun, Y. Yin, B. T. Mayers, T. Herricks and Y. Xia, *Chem. Mater* 2002, 1**4**, 4736-4745.

10. J. Jiu, T. Araki, J. Wang, M. Nogi, T. Sugahara, S. Nagao, H. Koga, K. Suganuma, E. Nakazawa and M. Hara, *J. Mater. Chem. A* 2014, **2**, 6326-6330.

11. Y. Shi, H. Li, L. Chen and X. Huang, *Sci.Technol. Adv. Mater* 2005, **6**, 761-765.

12. M. Mohl, P. Pusztai, A. Kukovecz, Z. Konya, J. Kukkola, K. Kordas, R. Vajtai and P. M. Ajayan, *Langmuir* 2010, **26**, 16496-16502.

13. M. Jin, G. He, H. Zhang, J. Zeng, Z. Xie and Y. Xia, *Angew. Chem. Int. Ed.* 2011, **50**, 10560-10564.

14. Y. Chang, L. Lye and H. C. Zeng, *Langmuir* 2005, **21**, 3746-3748.

15. A. R. Rathmell, S. M. Bergin, Y. L. Hua, Z. Y. Li and B. J. Wiley, *Adv. Mater.* 2010, **22**, 3558-3563.

16. H. Guo, N. Lin, Y. Chen, Z. Wang, Q. Xie, T. Zheng, N. Gao, S. Li, J. Kang and D. Cai, *Sci. Rep* 2013, **3**.

17. D. Zhang, R. Wang, M. Wen, D. Weng, X. Cui, J. Sun, H. Li and Y. Lu, *J. Am. Chem. Soc.* 2012, **134**, 14283-14286.

18. J. Sun, Y. Cheng, S. Wang, R. Wang and L. Gao, *J. Mater. Chem. C* 2014, **2**, 5309-5346.

19. S. Li, Y. Chen, L. Huang and D. Pan, *Inorg. Chem.* 2014, **53**, 4440-4444.

20. S. Mourdikoudis and L. M. Liz-Marzán, *Chem. Mater.* 2013, **25**, 1465-1476.

21. M. Chen, Y.-G. Feng, X. Wang, T.-C. Li, J.-Y. Zhang and D.-J. Qian, *Langmuir* 2007, **23**, 5296-5304.

22. M. Grzelczak, J. Pérez-Juste, P. Mulvaney and L. M. Liz-Marzán, *Chem. Soc. Rev.* 2008, **37**, 1783-1791.

23. C. J. Murphy, T. K. Sau, A. M. Gole, C. J. Orendorff, J. Gao, L. Gou, S. E. Hunyadi and T. Li, *J. Phys. Chem. B* 2005, **109**, 13857-13870.

24. B. Wiley, Y. Sun and Y. Xia, *Acc. Chem. Res.* 2007, **40**, 1067-1076.

25. N. Ortiz and S. E. Skrabalak, *Langmuir* 2014, *30*, 6649-6689.

26. F. Meng and S. Jin, *Nano Lett.* 2011, **12**, 234-239.

27. C. Mayousse, C. Celle, A. Carella and J.-P. Simonato, *Nano Res.* 2014, **7**, 315-324.

28. H.-J. Yang, S.-Y. He and H.-Y. Tuan, *Langmuir* 2013, **30**, 602-610.

29. K. C. Pradel, K. Sohn and J. Huang, *Angew. Chem. Int. Ed.* 2011, **50**, 3412-3416.

30. Y. Zheng, J. Zeng, A. Ruditskiy, M. Liu and Y. Xia, *Chem. Mater.* 2014, **26**, 22-33.

31. H.-J. Yang, S.-Y. He, H.-L. Chen and H.-Y. Tuan, *Chem. Mater.* 2014, **26**, 1785-1793.

32. J. Urban, H. Sack-Kongehl, K. Weiss, I. Lisiecki and M. P. Pileni, *Cryst. Res. Technol.* 2000, **35**, 731-743.

33. J. L. Elechiguerra, J. Reyes-Gasga and M. J. Yacaman, *J. Mater. Chem.* 2006, **16**, 3906-3919.

34. Y. Gao, L. Song, P. Jiang, L. Liu, X. Yan, Z. Zhou, D. Liu, J. Wang, H. Yuan and Z. Zhang, *J. Cryst. Growth* 2005, **276**, 606-612.

35. C. Ni, P. A. Hassan and E. W. Kaler, *Langmuir* 2005, **21**, 3334-3337.
36. Y. Sun, B. Mayers, T. Herricks and Y. Xia, *Nano Lett.* 2003, **3**, 955-960.
37. B. Nikoobakht and M. A. El-Sayed, *Langmuir* 2001, **17**, 6368-6374.
38. J. P. Vivek and I. J. Burgess, *Langmuir* 2012, **28**, 5040-5047.
39. J. P. Vivek and I. J. Burgess, *Langmuir* 2012, **28**, 5031-5039.
40. W. A. Al-Saidi, H. Feng and K. A. Fichthorn, *Nano Lett.* 2011, **12**, 997-1001.
41. Y. Gao, P. Jiang, D. F. Liu, H. J. Yuan, X. Q. Yan, Z. P. Zhou, J. X. Wang, L. Song, L. F. Liu, W. Y. Zhou, G. Wang, C. Y. Wang, S. S. Xie, J. M. Zhang and D. Y. Shen, *J. Phys. Chem. B* 2004, **108**, 12877-12881.
42. M. Grzelczak, J. Pe´rez-Juste, P. Mulvaney and L. M. Liz-Marza´n, *Chem. Soc. Rev.* 2008, **37**,1783-1791.
43. L. Gou, M. Chipara, and J. M. Zaleski, *Chem. Mater.* 2007, **19**, 1755-1760.
44. D. M. Grant and R. Kollrack, *J. Inorg. Nucl. Chem.* 1961, **23**, 25-29.
45. J. Bjerrum, C. Ballhausen and C. Jorgensen, *Acta Chem. Scand.* 1954, **8**, 1275-1289.
46. S. F. A. Kettle, *In Physical Inorganic Chemistry, Springer Berlin Heidelberg*: 1996; pp 156-184.
47. J. K. Cooper, A. M. Franco, S. Gul, C. Corrado and J. Z. Zhang, *Langmuir* 2011, **27**, 8486-8493.
48. A. Manna, T. Imae, M. Iida and N. Hisamatsu, *Langmuir* 2001, **17**, 6000-6004.

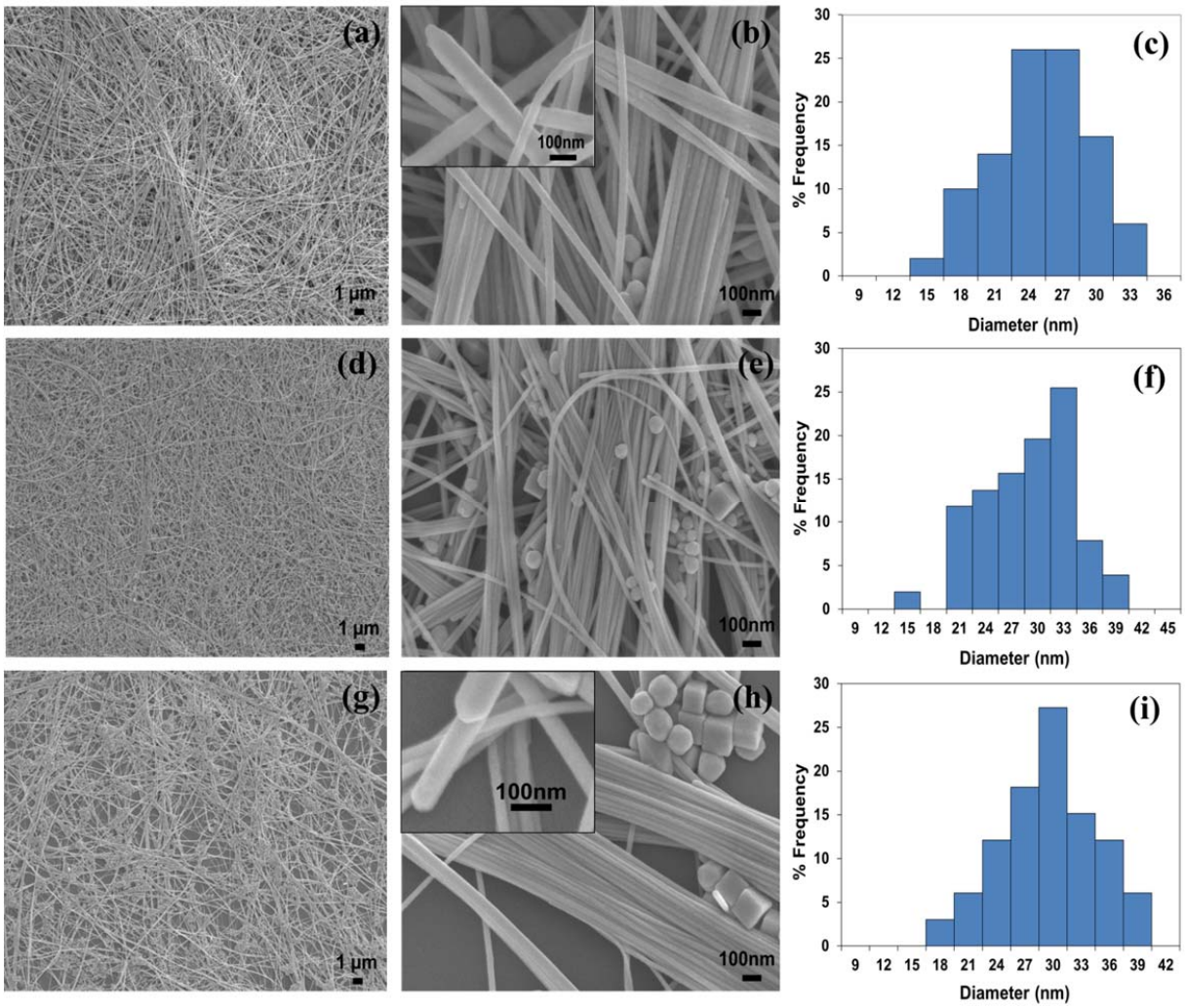


**Fig. 1** FESEM images of Cu nanowires synthesized using (a-b) HDA, (d-e) ODA, and (g-h) OLA. The particle diameter distributions of the corresponding nanowires synthsized using HDA, ODA, and OLA are shown in (c), (f), and (i), respectively. The insets in Fig.s 1b and 1h show side views of the nanowires with pentagonal ends.

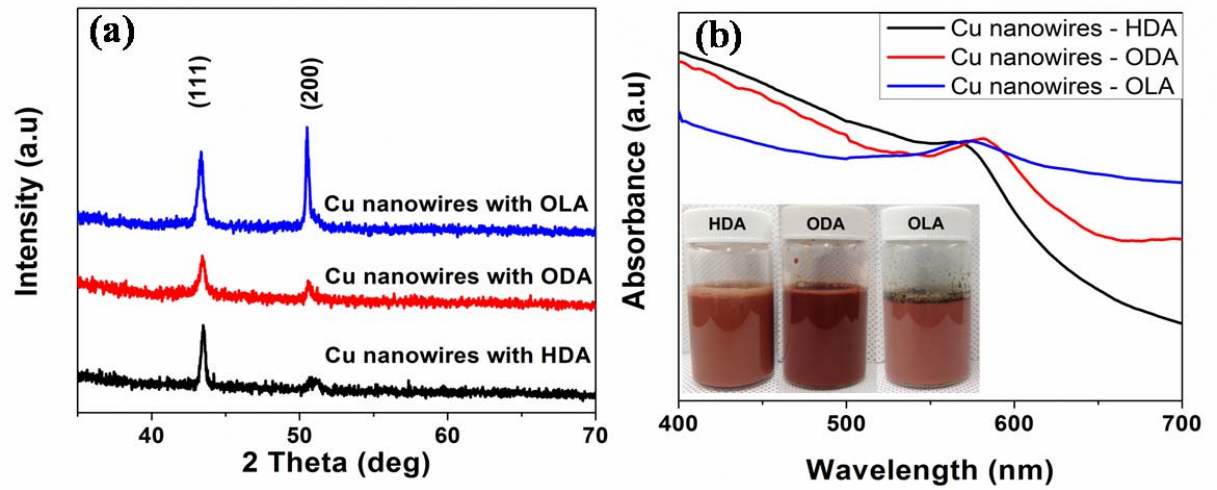


**Fig. 2** (a) XRD patterns of Cu nanowires synthesized using either HDA (black line), ODA (red line), or OLA (blue line). (b) UV-visible spectra of Cu nanowires to confirm the surface plasmon resonances where the image in the inset shows a photograph of the as-synthesized Cu nanowire dispersions.

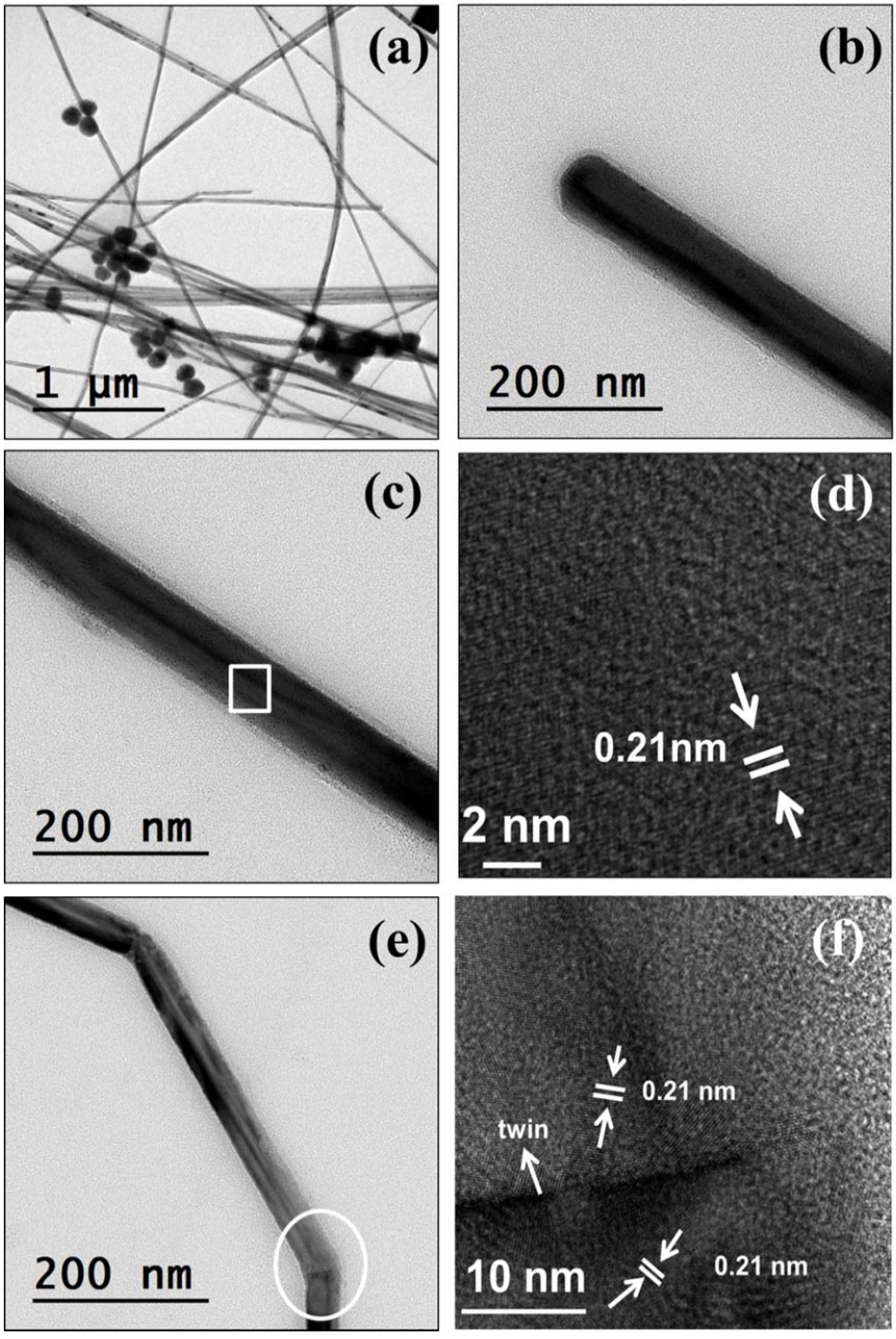


**Fig. 3** (a) HRTEM images of Cu nanowires synthesized using HDA. (b) Magnified image of the end portion of a nanowire. (c) Magnified image of the stem portion of a nanowire and (d) the corresponding high resolution image. The kinks present in the nanowire are shown in (e) and the magnified image of the encircled portion is shown in (f).

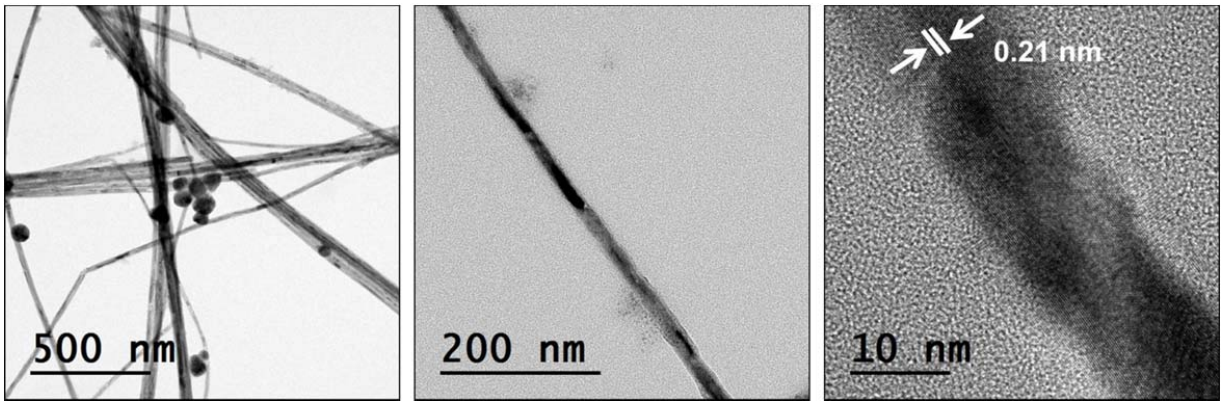


**Fig. 4** HRTEM images of Cu nanowires synthesized using ODA.

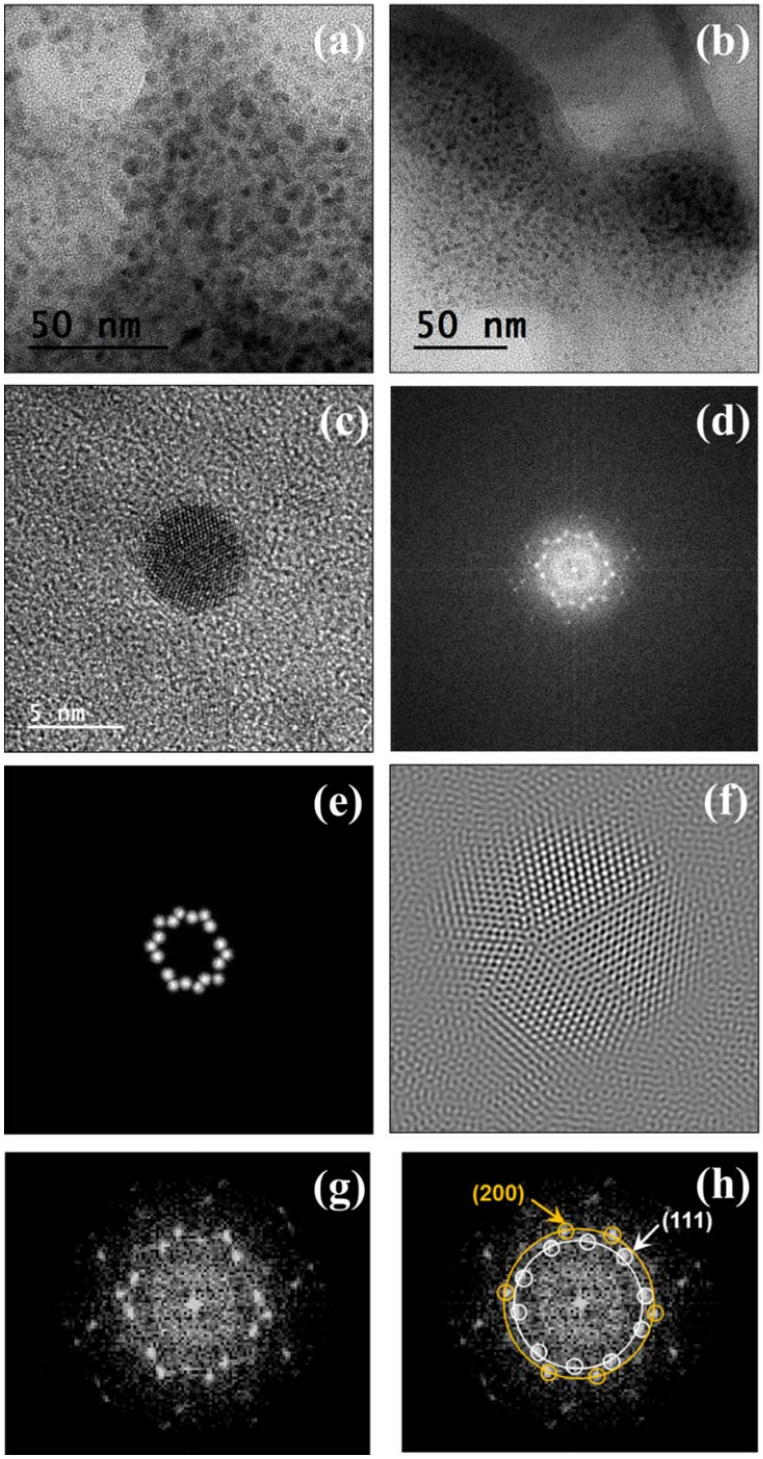


**Fig. 5** HRTEM images of the seeds formed at the initial stages of the reactions using either (a) HDA or (b) ODA confirming the penta-twinned nature of the seed particles. A magnified image of a single seed in the presence of HDA revealing the penta-twinned structure and the corresponding fast Fourier transform (FFT) are shown in (d). Fig. (e) and (f) show the masked pattern and inversed FFT, respectively, of the single seed particle shown in (c). The FFT of the single particle is magnified and indexed in (g) and (h), respectively. The image analysis reveals the (111) and (200) planes of the copper seed particles.

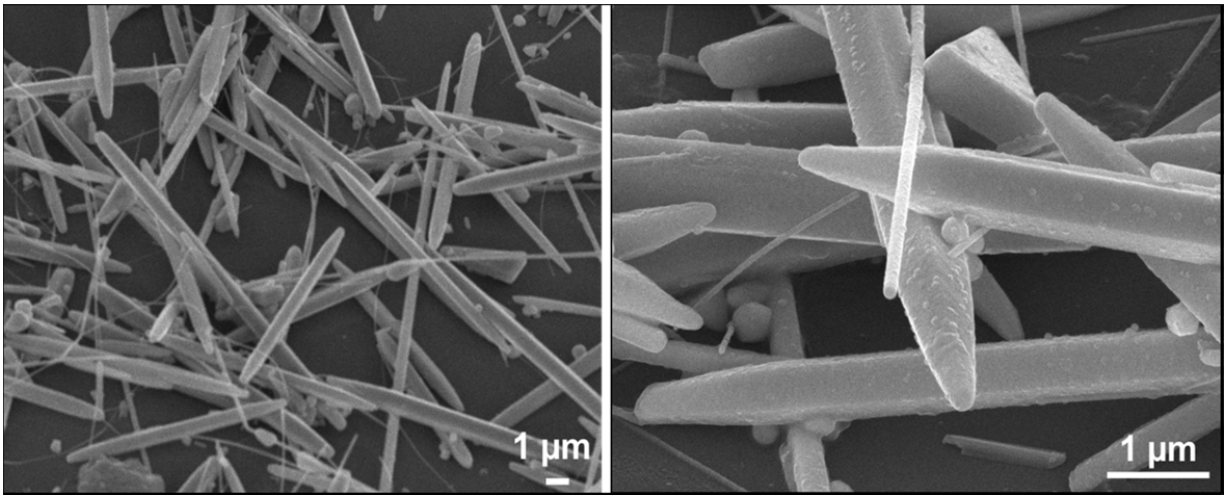


**Fig. 6** FESEM images of pencil-like micron-sized Cu rods synthesized with a low concentration of HDA.

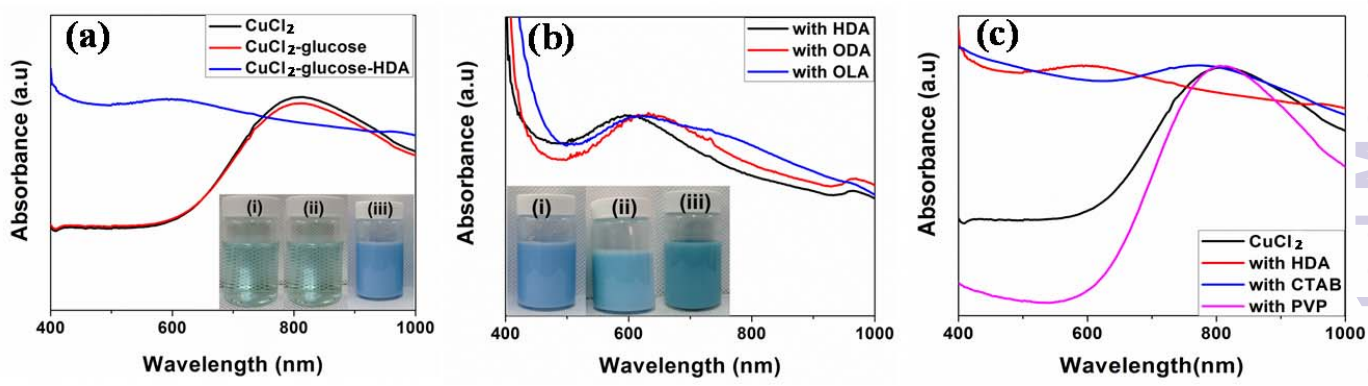


**Fig. 7** (a) UV-visible spectra and photographs of the samples of the (i) $CuCl_2$ solution (black line), (ii) $CuCl_2$ solution with glucose (red line), and (iii) $CuCl_2$ solution with glucose and HDA (blue line). (b) UV-visible spectra and photographs of the samples of the $CuCl_2$ solution with (i) HDA (black line), (ii) ODA (red line), and (iii) OLA (blue line). (c) UV-visible spectra of the $CuCl_2$ solution (black line) and $CuCl_2$ with HDA (red line), CTAB (blue line), and PVP (claret line).

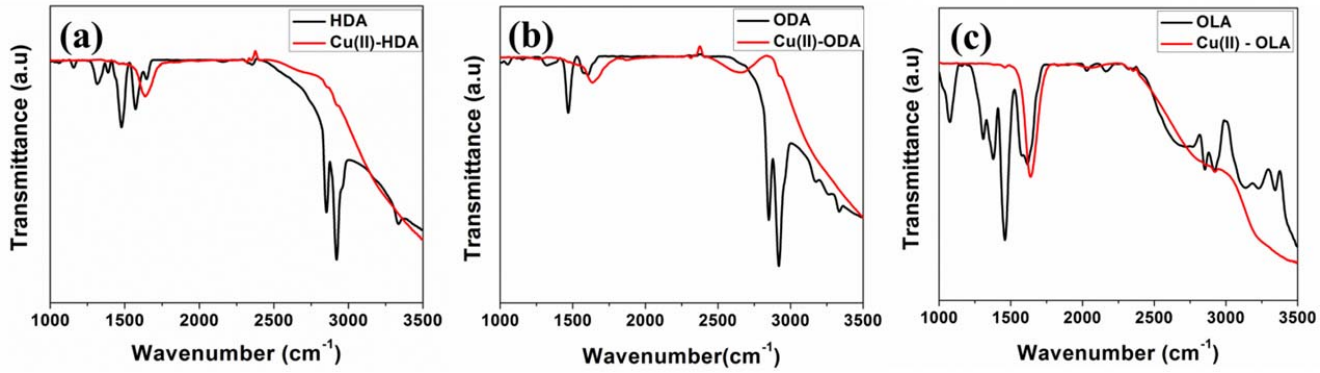


**Fig. 8** FT-IR spectra of free alkyl amines (black line) and their complexes of $Cu^{2+}$ ions (red line) with either (a) HDA, (b) ODA, or (c) OLA.

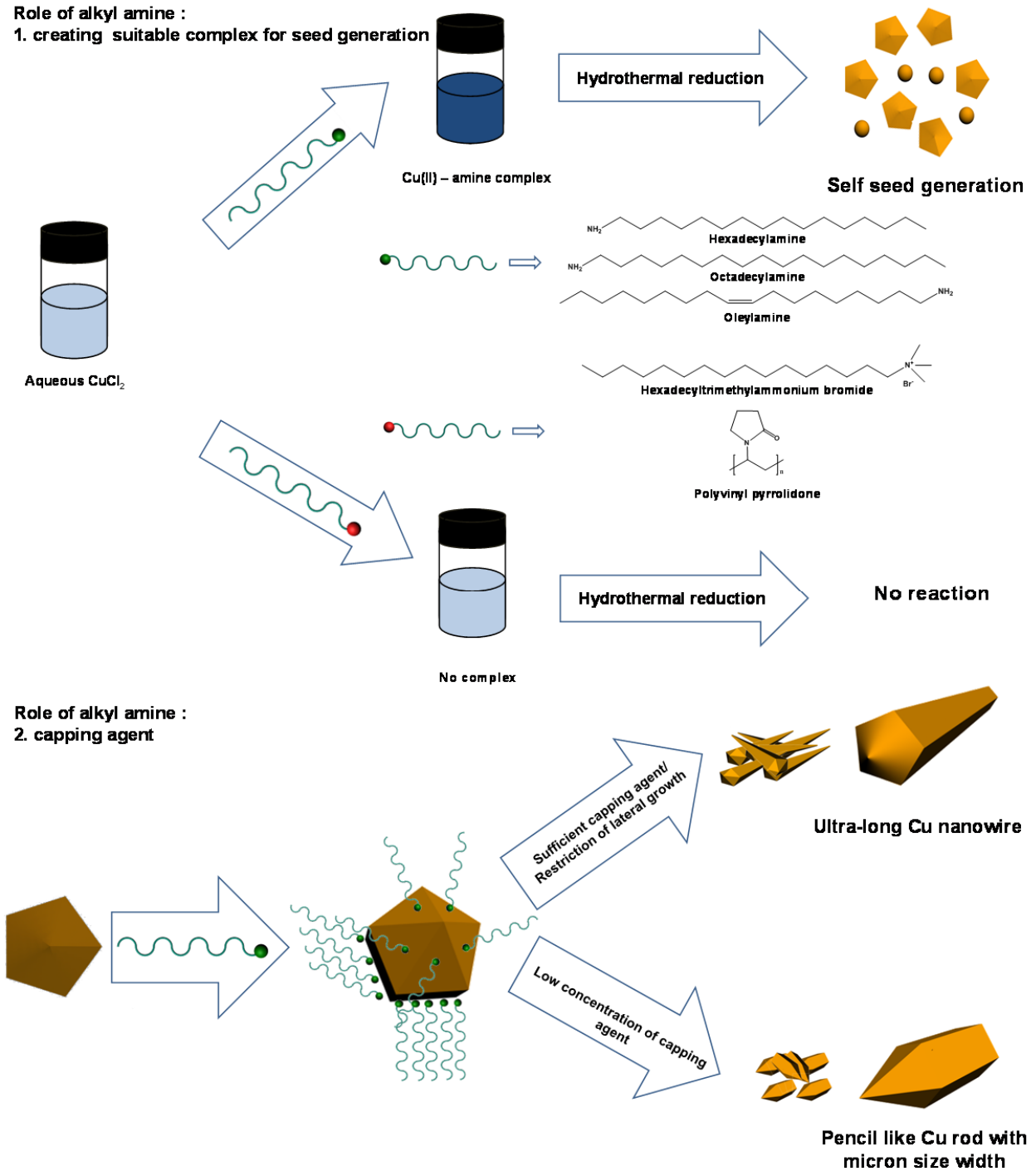


**Fig. 9** Schematic representation of the dual role of alkyl amines in the synthesis of Cu nanowires.

## GRAPHIC ABSTRACT

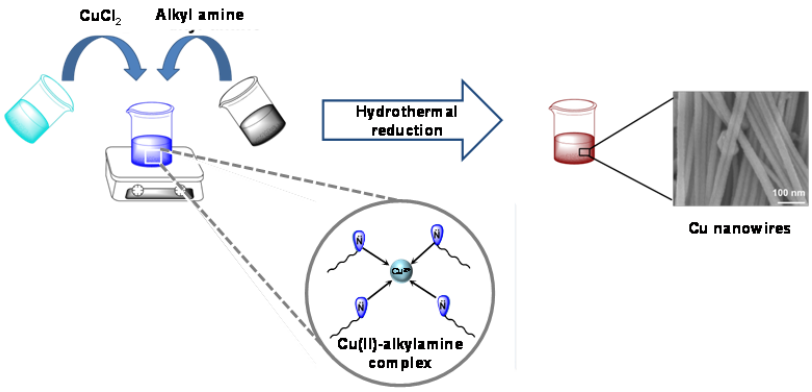


The complex formation of $Cu^{2+}$ ions with alkyl amines is a prerequisite for Cu nanowire synthesis. Slow reduction of this complex allows for the generation of twinned seeds which are later grown to nanowires.